6
Second-order Ripple in a DC Microgrid

In the previous Chapters, a stand-alone DC-DC-AC converter and quasi-switched boost inverter have been considered. In this Chapter, a detailed analysis of the $2\omega-$ripple is carried-out in the perspective of DC microgrid. In a typical DC microgrid, the sources, loads and storage are interconnected through the power converters. In this work, multiple DC-DC converters and inverter loads are considered. The DC-DC converters are considered for the upstream side and inverter loads are considered at the downstream side. A detailed modeling of the converters in the context of the second-order ripple is presented. The modeling is carried-out in the small-signal sense. The inverter loads inject the $2\omega-$ripples at the DC-bus through downstream converters and these ripples further propagate towards DC sources through the upstream converters and get injected into the sources. Furthermore, a phase-adjustment based $2\omega-$ripple minimization technique is discussed using the two inverter loads. The chapter begins with the derivation of second-order ripple in DC link current in the small signal sense in the Section 6.1. The development of equivalent circuit of an individual DC-DC converter with inverter load using small signal model is discussed in Section 6.2. In the Section 6.3, the ripple analysis for an island DC Microgrid is carried-out using the equivalent circuits of different converters within the DC microgrid. In the Section 6.4, the simulation results are presented and the effect of different system parameters on the $2\omega-$ripple is investigated through the Bode plot technique. In the Section 6.5, the phase-adjustment based $2\omega-$ripple minimization technique is discussed. The Section 6.6, summarizes the Chapter Six.

6.1 DERIVATION OF SECOND-ORDER RIPPLE IN SMALL SIGNAL SENSE

Suppose v_{ac} and i_{ac} are the instantaneous output voltage and output current of the inverter, then the instantaneous output power of inverter is,

$$p_{ac} = v_{ac}i_{ac} = V_{max}cos(\omega t)I_{max}cos(\omega t-\theta) \tag{6.1a}$$

$$= \frac{V_{max}I_{max}}{2}[cos\theta(1+cos2\omega t)+sin\theta(sin2\omega t)] \tag{6.1b}$$

Here v_{ac} and i_{ac} are the instantaneous values of output voltage and output current of inverter respectively. *max* represents the maximum value. Clearly, the instantaneous power contains ripple power component pulsating at 2ω rad/sec over the average DC value of power. For simplicity, suppose the power factor angle (θ) is zero. This reduces (6.1),

$$p_{ac} = \frac{P_{max}}{2}(1+cos2\omega t) \tag{6.2a}$$

$$= \frac{P_{max}}{2}+\frac{P_{max}}{2}cos2\omega t \tag{6.2b}$$

Here, $P_{max} = V_{max}I_{max}$. Suppose V_o is the average DC voltage and I_o is the average DC current at the input of the inverter. $\tilde{v_o}$ and $\tilde{i_o}$ are the corresponding ripple components pulsating over the average values. The instantaneous input power of inverter is,

$$p_{dc} = (V_o+\tilde{v_o})(I_o+\tilde{i_o}) \tag{6.3a}$$

$$= V_oI_o+V_o\tilde{i_o}+I_o\tilde{v_o}+\tilde{v_o}\tilde{i_o} \tag{6.3b}$$

In small signal sense, the voltage ripple ($\tilde{v_o} << V_0$) and cross-product term ($\tilde{v_o}\tilde{i_o}$) can be neglected. For an ideal inverter, input DC power is equal to output AC power. Considering these in (6.2) and (6.3), gives the current ripple component ($\tilde{i_o}$)

$$\tilde{i_o} = \frac{P_{max} cos(2\omega t)}{2V_o} \tag{6.4}$$

The Laplace transform of (6.4) gives,

$$\tilde{i_o}(s) = \frac{P_{max}}{2V_o}\left(\frac{s^2}{s^2+4\omega^2}\right) \tag{6.5}$$

The angular frequencies 100π rad/sec and 120π rad/s are used worldwide for the electrical power supply. Therefore, the ripple frequencies are 200π rad/sec and 240π rad/sec respectively. For the 100 rad/sec, the equation (6.5) gives,

$$\tilde{i_o}(s)|_{\omega=100\pi(rad/s)} = \frac{P_{max}}{2V_o}\left(\frac{s^2}{s^2+394784.17}\right) \tag{6.6}$$

The focus of this work is to carry-out a study on the SHC ripple in perspective of the typical island DC microgrid. In a microgrid, the sources, loads and storage are interconnected through power converters in general. To conduct analytic study on the microgrid, a model of the complete system is required. In this work, the analysis is carried out using small signal model of microgrid. However, instead of going directly for the development of complete equivalent model/circuit of DC microgrid, for the sake of simplicity and better understanding, an example of the design procedure for the equivalent circuit of a boost-derived DC-DC converter with inverter load will be discussed. Secondly, the relation between the current ripple reflected at the input of inverter and the current ripple injected into the DC source through front end converter circuit will be deduced.

6.2 DEVELOPMENT OF EQUIVALENT CIRCUIT

In this Section, the basic idea of the development of equivalent circuit of a converter through its small signal model is discussed. The steps followed are: design of nonlinear large signal model, conversion of large signal nonlinear model in small signal nonlinear model using perturbation method, reduction of small signal nonlinear model in linear AC model in time domain, transformation of time domain AC model in $s-$domain AC model using Laplace transform and development of equivalent circuit using $s-$domain AC model.

6.2.1 Large Signal Average Model

The circuit diagram of a boost converter feeding inverter load is shown in Fig. 6.1. In Fig. 6.1, x_1, x_2, x_3 are input current, inductor current, and load current. y_1 and y_2 are voltage across input capacitor and voltage across output capacitor; u is control input. L is inductance, and C_{in} is input capacitance and C_o is the output capacitance. E is the EMF of source. r_{in} and r_L are source and inductor parasitic resistances. The inverter load is modeled using current source as shown in Fig. 6.1. The instantaneous large signal average model of boost converter is,

$$C_{in}\dot{y}_1 = x_1 - x_2 \tag{6.7a}$$
$$C_o\dot{y}_2 = (1-u)x_2 - x_3 \tag{6.7b}$$
$$L\dot{x}_2 = y_1 - r_L x_2 - (1-u)y_2 \tag{6.7c}$$

6.2.2 Linear Equivalent Circuit

A small signal nonlinear model is designed from the nonlinear average model of boost converter. This is achieved by perturbing state variables about steady state variables. The state

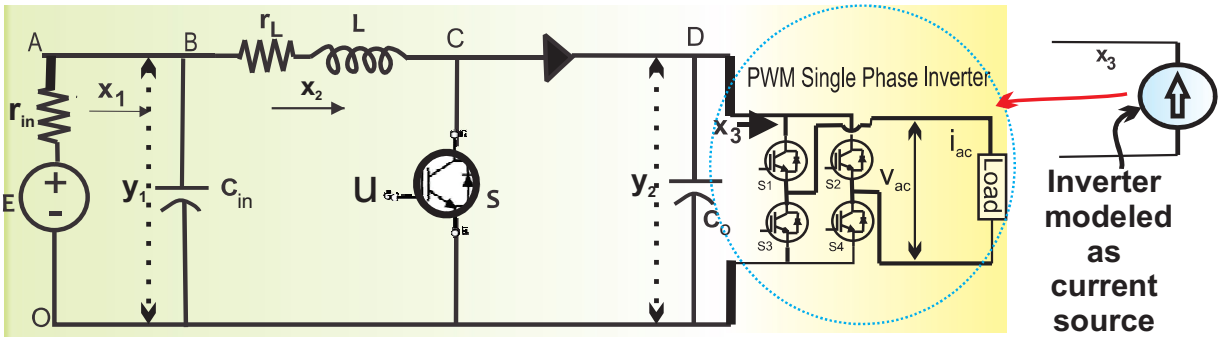

Figure 6.1 : Two-stage DC-DC-AC boost converter

variables with small signal perturbation are given in (6.8).

$$x_1 : = I_{in} + \tilde{i_{in}} \tag{6.8a}$$
$$x_2 : = I_L + \tilde{i_L} \tag{6.8b}$$
$$x_3 : = I_o + \tilde{i_o} \tag{6.8c}$$
$$y_2 : = V_o + \tilde{v_o} \tag{6.8d}$$
$$y_1 : = E - r_{in}\tilde{i_{in}} \tag{6.8e}$$
$$u : = D + \tilde{d} \tag{6.8f}$$

Here, $I_{in}, E, I_L, V_o, I_o, D$ are steady state constant DC components and $\tilde{i_{in}}, \tilde{i_L}, \tilde{v_o}, \tilde{i_o}, \tilde{d}$ are small signal AC ripple components of the variable respectively. Using (6.7) and (6.8), a small signal nonlinear model is obtained. The DC steady-state terms and nonlinear cross-product terms are eliminated from small-signal model and only the first order AC linear terms are collected together. This gives a small signal linear AC model of boost converter as follows,

$$-C_{in}r_{in}\dot{\tilde{i_{in}}} = \tilde{i_{in}} - \tilde{i_L} \tag{6.9a}$$
$$C_o\dot{\tilde{v_o}} = D'\tilde{i_L} - I_L\tilde{d} - \tilde{i_o} \tag{6.9b}$$
$$L\dot{\tilde{i_L}} = -r_{in}\tilde{i_{in}} - r_L\tilde{i_L} + V_o\tilde{d} - D'\tilde{v_o} \tag{6.9c}$$

The current ripple reflected at the input of inverter is $\tilde{i_o}$. Henceforth, the inverter will be represented by a current source injecting a current ripple $\tilde{i_o}$ (in small signal sense) at output of the DC-DC converter. For the analysis of SHC ripple, the frequency domain analysis is followed. This is why, the time domain model given by (6.9), is transformed into the s-domain using Laplace transform as follows.

$$-sC_{in}r_{in}\tilde{i_{in}}(s) = \tilde{i_{in}}(s) - \tilde{i_L}(s) \tag{6.10a}$$
$$sC_o\tilde{v_o}(s) = D'\tilde{i_L}(s) - I_L\tilde{d}(s) - \tilde{i_o}(s) \tag{6.10b}$$
$$sL\tilde{i_L}(s) = -r_{in}\tilde{i_{in}}(s) - r_L\tilde{i_L}(s) + V_o\tilde{d}(s) - D'\tilde{v_o}(s) \tag{6.10c}$$

Further, this s-domain model is used to develop the equivalent circuit. The development of equivalent circuit is shown in Fig. 6.2(a)-(b).

6.2.3 Calculation of Current Ripple Injected at Input

In Fig. 6.2(b), it should be noted that $\tilde{i_o}(s)$ distributes at the different nodes depending on the impedance of the corresponding branch(s). The AC equivalent circuit facilitates to calculate the components of $\tilde{i_o}(s)$ injected at source and different nodes in the circuit. It is worth noting that, hereafter, the AC ripple is considered SHC ripple only; prime focus is the analysis of second-order

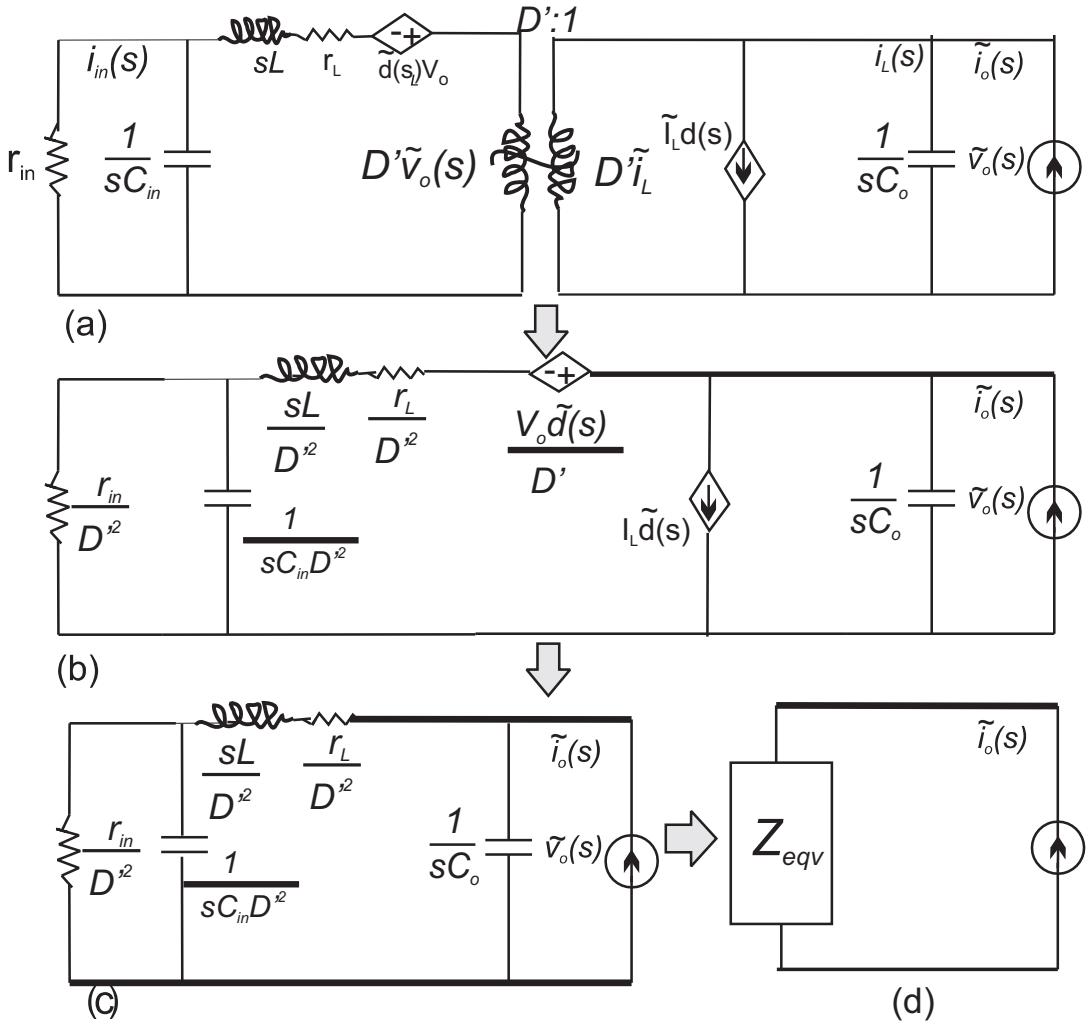

Figure 6.2 : (a) canonical form of linear boost converter model (b) equivalent circuit (c) reduced circuit at fixed duty, $\tilde{d}(s) = 0$ (d) single port model

ripple. For the ripple analysis, a relation between current ripple $\tilde{i_o}(s)$ reflected by inverter load at the input of inverter and injected current ripple, $\tilde{i_{in}}(s)$ into DC source through boost converter in terms of system parameters ($C_{in}, C_o, L, r_{in}, r_L$ etc) will be deduced. The analysis is carried-out for the open loop configuration, that is a fixed duty cycle operation. This implies $\tilde{d}(s) = 0$. This implies that in Fig. 6.2(b), the sources dependent on $\tilde{d}(s)$ one eliminated. This reduces the circuit of Fig.6.2(b) into the reduced equivalent circuit as shown in the Fig.6.2(c). The current ripple, $\tilde{i_o}(s)$ at the DC link propagates towards the source and distributes at the different nodes of the boost converter, and eventually get injected into the DC source. In the circuit of Fig.6.2(c), suppose $Z_{in} = \frac{r_{in}}{D'^2}, Z_{C_{in}} = \frac{1}{sC_{in}D'^2}, Z_L = \frac{(r_L+sL)}{D'^2}$ and $Z_{C_o} = \frac{1}{sC_o}$. Using current distribution method, we have

$$\tilde{i_{in}}(s)|_{\tilde{d}(s)=0} = \Big(\frac{Z_{C_o}Z_{C_{in}}}{(Z_{C_o} + Z_L + \frac{Z_{in}Z_{C_{in}}}{Z_{in}+Z_{C_{in}}})(Z_{in} + Z_{C_{in}})}\Big)\tilde{i_o}(s) \tag{6.11a}$$

$$\tilde{i_{in}}(s)|_{\tilde{d}(s)=0} = \lambda(s)\tilde{i_o}(s) \tag{6.11b}$$

Here, $\lambda(s) = D'^2(r_{in}LC_{in}C_os^3 + C_o(L + r_Lr_{in}C_{in})s^2 + (C_o(r_{in} + r_L) + r_{in}C_{in}D'^2)s + D'^2)^{-1}$.
The circuit of Fig. 6.2(c) is further reduced in single-port network as shown in Fig. 6.2(d). In single-port network, the Z_{eqv} is,

$$Z_{eqv}(s) = \frac{r_{in}C_{in}Ls^2 + (L + r_{in}r_LC_{in})s + r_{in} + r_L}{r_{in}LC_{in}C_os^3 + C_o(L + r_Lr_{in}C_{in})s^2 + (C_o(r_{in} + r_L) + r_{in}C_{in}D'^2)s + D'^2} \tag{6.12}$$

The ripple power drawn by $Z_{eqv}(s)$ in the circuit of Fig. 6.2(d) is,

$$P_{SHC}(s) = Z_{eqv}(s)\tilde{i}_o^2(s) \tag{6.13}$$

It is to be noted that the low-frequency $2\omega-$power ripple (given by (6.13)) causes an increase in the rated peak power and this leads to increase in the size of the components and their rating in the system. This concludes that the SHC ripple increases the rating of the source and power electronics components.

The same procedure can be followed to develop equivalent circuit of the other converters like buck converter, isolated bidirectional buck-boost, impedance-source converters etc. The equation (6.11) relates the reflected current ripple at input of inverter and injected current ripple at source. This relation will be used for analysis in the following section. In the next Section, the procedure for the development of equivalent circuit for a typical DC microgrid in small signal sense is presented.

6.3 RIPPLE ANALYSIS FOR ISLAND DC MICROGRID

A diagram of a typical island DC microgrid is shown in the Fig.6.3(a). There are $n-$upstream side converters (USCs) and $m-$downstream side converters (DSCs) connected to DC bus. For the simplicity, the non-isolated buck converter and boost converter topologies are considered. However, one may also choose different converter topologies for similar analysis.

In Fig. 6.3(a), the DC sources are connected to DC bus through upstream side DC-DC boost converter. The battery bank is connected to DC bus through bi-directional converter. The DC bus supplies power to inverter loads through downstream side DC-DC buck converters. Some inverter loads, those operate at relatively higher voltage, are directly connected to the DC bus *say* DCI. The boost converters are generally used to integrate low voltage distributed generators to DC bus. A bi-directional DC-DC converter interfaces the battery and DC bus and exchanges power. During power deficit in DC microgrid, the bi-directional converter works as boost converter. In such case, a typical DC-DC boost converter and a DC-DC bi-directional converter have similar circuit topology.

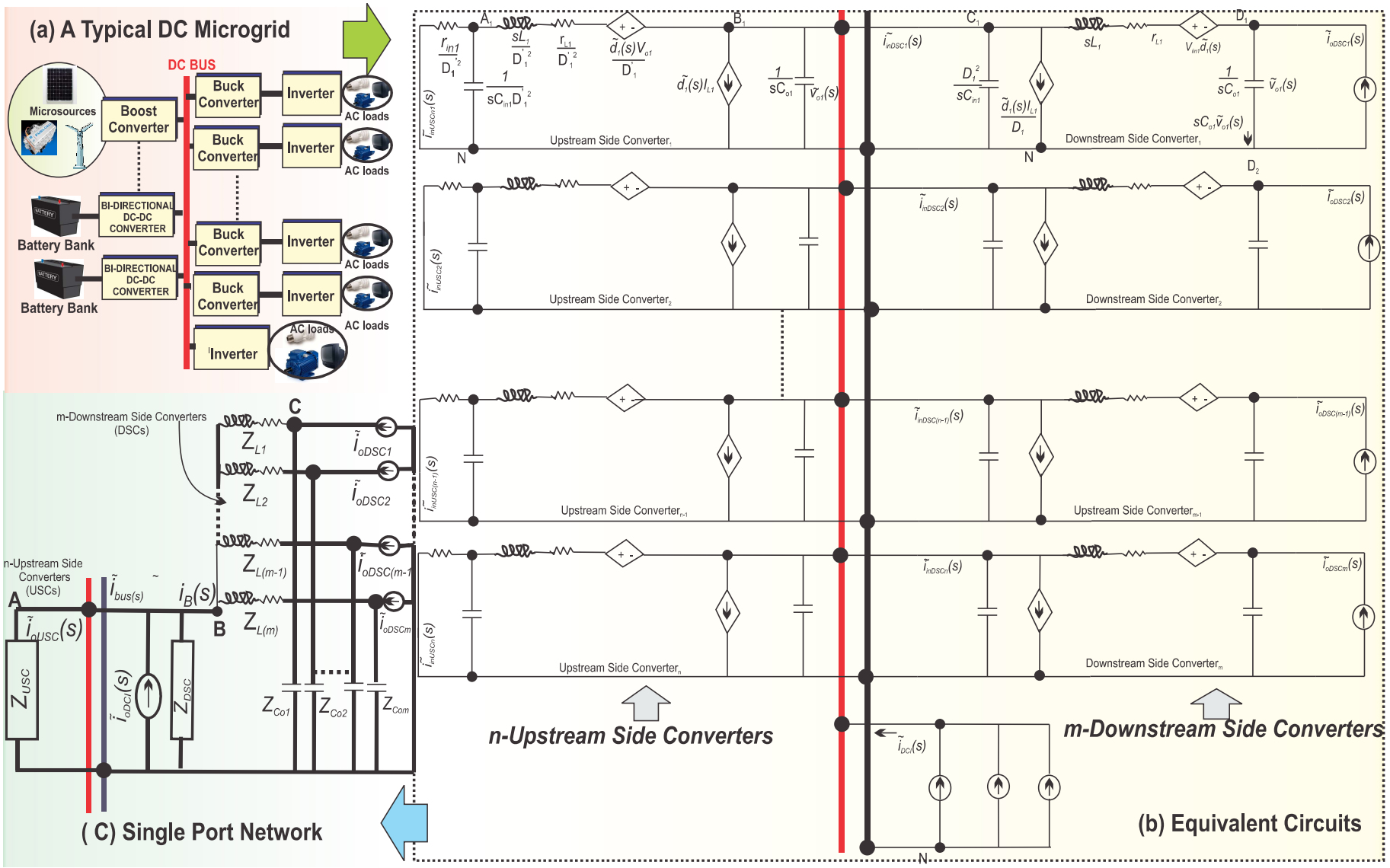

Figure 6.3 : (a) A typical Island DC microgrid (b) linear small signal circuit (c) single port network

Also, in the boost operation mode, the bi-directional converter supplies power to inverter load only. The battery bank is charged in buck mode by DC sources. Here, this is emphasized that the analysis carried-out in this work has considered island DC microgrid containing DC source only, nonetheless, the main focus of this work is to study the impact of the SHC ripple on the DC microgrid having single-phase inverter loads. This SHC ripple is reflected when DC source exchanges power through AC-DC converter.

The equivalent circuits of each converter of DC microgrid are shown in Fig.6.3(b). The ripple reflects at the DC input of inverter and propagates to the DC bus through front-end DC-DC converter (if any). The ripple injected at the DC bus distributes among the upstream converters. Using equivalent circuit in the Fig. 6.3(c), firstly (i) the relation between current ripple reflected at input of inverter and current ripple injected into DC bus will be deduced and secondly (ii) the relation between current ripple injected at bus and current ripple injected into DC sources will be deduced.

6.3.1 Ripple Injected into DC Bus by Down Stream Inverter loads

A simplified single port network of the Fig. 6.3(b) is shown in Fig. 6.3(c). In Fig. 6.3(c), Z_{USC} is the lumped impedance seen at the DC bus in the direction of the sources. The equivalent impedance of each USC converter seen at the DC bus in the direction of its source is calculated (similar to (6.11)) as follows,

The equivalent impedance of k^{th} upstream side converter is,

$$Z_{USC_k} = \frac{r_{in_k}C_{in_k}L_k s^2 + (L_k + r_{in_k}r_{L_k}C_{in_k})s + r_{in_k} + r_{L_k}}{r_{in_k}L_kC_{in_k}C_{o_k}s^3 + C_{o_k}(L_k + r_{L_k}r_{in_k}C_{in_k})s^2 + (C_{o_k}(r_{in_k} + r_{L_k}) + r_{in_k}C_{in_k}{D'_k}^2)s + {D'_k}^2} \tag{6.14}$$

All the upstream side converters are connected in parallel at the DC bus. Suppose Z_{USC} is the equivalent impedance of the upstream converters. Using (6.14), the value of Z_{USC} is,

$$Z_{USC} = (\sum_{k=1}^{n} \frac{1}{Z_{USC_k}})^{-1} \tag{6.15}$$

In the Fig. 6.3(c), suppose Z_{DSC} is the equivalent impedance of input capacitors of the downstream converters connected in parallel at the DC bus and in the Fig. 6.3(c), the impedance of the j^{th} input capacitor is $Z_{DSC_j} = \frac{{D_j}^2}{sC_{in_j}}$ and therefore,

$$Z_{DSC} = (\sum_{j=1}^{m} \frac{1}{Z_{DSC_j}})^{-1} \tag{6.16}$$

Now suppose the impedance of inductor and output capacitor of j^{th} downstream side converter (see Fig. 6.2(c)) are $Z_{L_j} = (r_{L_j} + sL_j)$ and $Z_{C_{o_j}} = \frac{1}{sC_{o_j}}$ respectively. Using current distribution method in the circuit of Fig. 6.3(c), the current ripple injected at node 'B' by j^{th} converter is calculated i.e.,

$$\tilde{i}_{B_j}(s) = \gamma_j \tilde{i}_{oDSC_j}(s) \tag{6.17}$$

Here, $\gamma_j = \frac{Z_{C_{o_j}}}{Z_{L_j} + Z_{C_{o_j}} + (\frac{Z_{USC}Z_{DSC}}{Z_{USC}+Z_{DSC}})}$. Also, the ripple injected at node 'B' by directly connected inverter (DCI) loads is $\tilde{i}_{o_{DCI}}(s)$ (see Fig. 6.3(c)). This gives the total ripple injected at node 'B',

$$\tilde{i}_{B_{Total}}(s)|_{\tilde{d}(s)=0} = \tilde{i}_{o_{DCI}}(s) + \sum_{j=1}^{m} \tilde{i}_{B_j}(s) \tag{6.18}$$

Using the current distribution, the current injected at DC bus can be calculated as follows,

$$\tilde{i}_{bus}(s) = \Big(\frac{Z_{DSC}}{Z_{USC}+Z_{DSC}}\Big)\tilde{i}_{B_{Total}}(s)|_{\tilde{d}(s)=0} \tag{6.19}$$

Using (6.5), (6.18) and (6.19), the ripple injected at DC bus by downstream side converter is,

$$\tilde{i}_{bus}(s) = \Big(\frac{Z_{DSC}}{Z_{USC}+Z_{DSC}}\Big)\Big(\frac{s^2}{s^2+4\omega^2}\Big)\Big(\frac{P_{max_{DCI}}}{2V_{bus}} + \sum_{j=1}^{m}\frac{\gamma_j P_{max_j}}{2V_{o_j}}\Big) \tag{6.20}$$

Here, $\frac{P_{max_j}}{2}$ is the active power of the j^{th} downstream side converter-fed inverter load. $\frac{P_{max_{DCI}}}{2}$ is the active power of the directly connected inverter loads to DC bus.

6.3.2 Ripple Injected into DC Sources by DC Bus

As all the upstream converters are connected in parallel to common DC bus, the total current ripple injected at DC bus ($\tilde{i}_{bus}(s)$) distributes among different converters at upstream side depending on their equivalent impedance. The component of $\tilde{i}_{bus}(s)$ that is injected at the output of k^{th} upstream converter by DC bus is given by,

$$\tilde{i}_{o_{USC_k}}(s)|_{\tilde{d}(s)=0} = \tilde{i}_{bus}(s)\frac{(\sum_{\substack{r=1\\r\neq k}}^{n}\frac{1}{Z_{USC_r}})^{-1}}{Z_{USC_k}+(\sum_{\substack{r=1\\r\neq k}}^{n}\frac{1}{Z_{USC_r}})^{-1}} \tag{6.21}$$

Now using (6.11), we can get relation between the current injected at the output of k^{th} upstream converter ($\tilde{i}_{o_{USC_k}}(s)$) and the current ripple at DC source, $\tilde{i}_{in_{USC_k}}(s)$ as follow,

$$\tilde{i}_{in_{USC_k}}(s)|_{\tilde{d}(s)=0} = \lambda_k(s)\tilde{i}_{o_{USC_k}}(s) \tag{6.22}$$

Using (6.20), (6.21) and (6.22), we get an important relation of the ripple injected into the k^{th} source through k^{th} USC converter in terms of the active power of inverters, nominal voltage of DC bus and system parameters as follows,

$$\tilde{i}_{in_{USC_k}}(s)|_{\tilde{d}(s)=0} = \Big(\frac{\lambda_k(s)Z_{DSC}}{Z_{USC}+Z_{DSC}}\Big)\Big(\frac{(\sum_{\substack{r=1\\r\neq k}}^{n}\frac{1}{Z_{USC_r}})^{-1}}{Z_{USC_k}+(\sum_{\substack{r=1\\r\neq k}}^{n}\frac{1}{Z_{USC_r}})^{-1}}\Big)\Big(\frac{s^2}{s^2+4\omega^2}\Big)\Big(\frac{P_{max_{DCI}}}{2V_{bus}} + \sum_{j=1}^{m}\frac{\gamma_j P_{max_j}}{2V_{o_j}}\Big) \tag{6.23}$$

From (6.21), the $\tilde{i}_{o_{USC_k}}(s)$ can be obtained. This is the SHC current that flows through different components of k^{th}-upstream side converter to source. This means an additional power given by (6.24) is required to supplies inverter loads.

$$P_{SHC_k} = Z_{USC_k}\left(\frac{(\sum_{\substack{r=1\\r\neq k}}^{n}\frac{1}{Z_{USC_r}})^{-1}}{Z_{USC_k}+(\sum_{\substack{r=1\\r\neq k}}^{n}\frac{1}{Z_{USC_r}})^{-1}}\tilde{i}_{bus}(s)\right)^2 \tag{6.24}$$

This implies that the total additional power ($P_{SHC_{Total}}$) needed to be supplied by sources connected to USC is, $\sum_{k=1}^{n} P_{SHC_k} = Z_{USC}\tilde{i}_{bus}^2(s)$, substituting (6.20) in this gives,

$$P_{SHC_{Total}} = \left[\Big(\frac{Z_{DSC}\sqrt{Z_{USC}}}{Z_{USC}+Z_{DSC}}\Big)\Big(\frac{s^2}{s^2+4\omega^2}\Big)\Big(\frac{P_{max_{DCI}}}{2V_{bus}} + \sum_{j=1}^{m}\frac{\gamma_j P_{max_j}}{2V_{oj}}\Big)\right]^2 \tag{6.25}$$

Now, suppose P_{eqv} is the total active power supplied by USCs at bus, then the power factor at DC bus is,

$$p.f. = \frac{P_{eqv}}{\sqrt{P_{eqv}^2 + P_{SHC_{Total}}^2}} \tag{6.26}$$

6.4 RESULTS

In this Section, the effect of the variations in the system parameters on the SHC ripple at the input is investigated through the Bode plot technique. The Fig 6.4 shows four Bode plots to relate the variation in the magnitude of second-order ripple in the input current at the source (i.e. equivalent second-order ripple current injected by the different inverter loads in DC microgrid given by equation 6.23) with respect to variations in the system parameters (which are inductance, capacitance and parasitic resistance) for different values of frequency. The equation given by (6.23) relates the SHC ripple in the input current of the k^{th} upstream converter with the system parameters. For this $\tilde{i}_{in_{USC_k}}(s)|_{\tilde{d}(s)=0}$ is plotted for the first upstream converter i.e. $k = 1$. Two upstream converters (i.e. $k = 1,\ 2$) and two downstream converters (i.e. $j = 1,\ 2$) feeding inverter load each of 1 kW are considered with one directly connected inverter load of 3 kW. The DC bus voltage (v_{bus}) is 380 V, the source voltages (E) are at 120 V and output voltages of downstream converter are at 220 V. For this study, the system parameters i.e. inductor, input capacitor, output capacitor, parasitic resistance of the inductor, internal resistance of the source and source voltage are chosen. The effect of the change in the values of the aforesaid system parameters on the $2\omega-$ripple in the input current of the first upstream converter is studied through the bode plot technique. For this, the values of the same parameter i.e. C_{in} or C_o or L or r_L of all converters (whether it is of downstream converter or of upstream converter) are varied simultaneously.

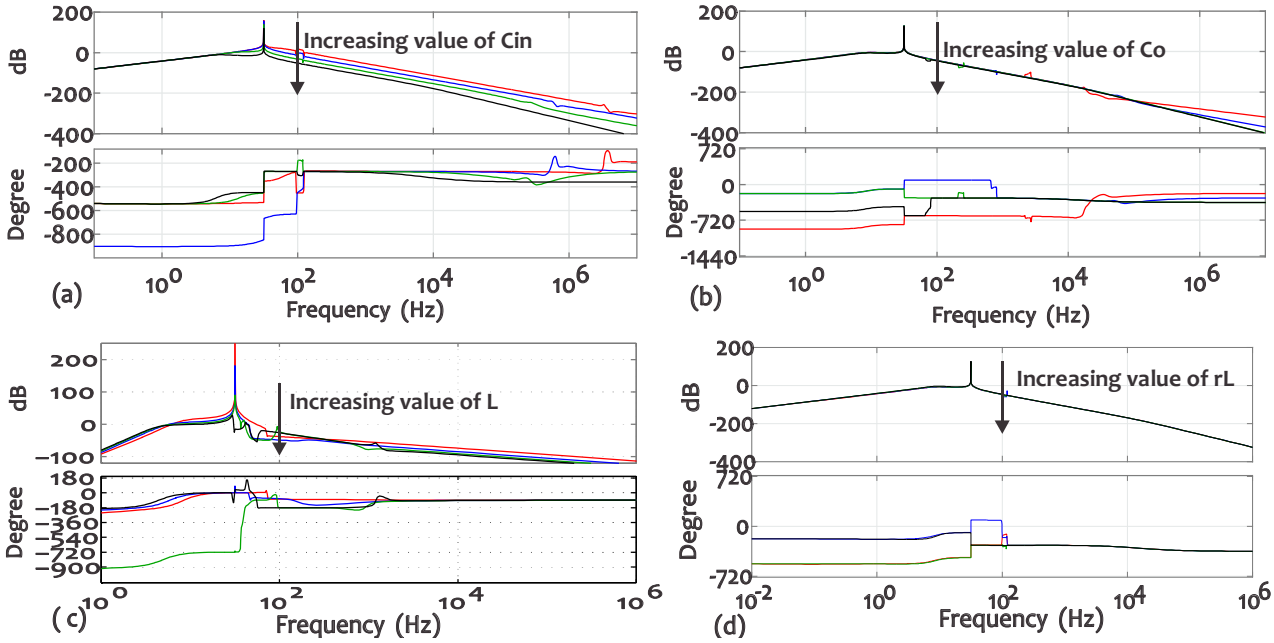

Figure 6.4 : Bode diagram of (6.23)

From the Fig. 6.4, it can be concluded that the variation in the values of the input capacitance (C_{in}) of the converters and variation in the values of inductance (L) of the converters affect the $2\omega-$ripple. Here the $2\omega-$ripple is of 100 Hz for inverters supplying AC loads at 50 Hz. The variation in the values of the output capacitance (C_o) of the converters and variation in the values of the parasitic resistance of the inductance (r_L) of converters cause negligible effect on the $2\omega-$ripple. With the increase in the values of the C_{in} and C_o cause decrease in the $2\omega-$ripple in the input current ($\tilde{i}_{in_{USC_{k=1}}}$) of the first source connected to the bus through upstream converter ($k = 1$).

The summary of the results shown in Fig. 6.4 is given in Table 6.1. In the Table 6.1, the system parameter (that is varied), the values of varying parameter and fixed parameters, the corresponding figure number in Fig. 6.4 and remark are listed.

Table 6.1 : Summary of Fig. 6.4

Parameter	Values	Figure	Remark
Variation in input capacitance of each converter (C_{in_k} and C_{in_j})	Variable parameter: $C_{in_{k=1}} = C_{in_{k=2}} = C_{in_{j=1}} = C_{in_{j=2}} = 2\mu F,\ 22\mu F,\ 0.22mF,\ 2.2mF$ Fixed parameters: $C_{o_{k=1}} = C_{o_{k=2}} = C_{o_{j=1}} = C_{o_{j=2}} = 1mF$ $r_{L_{k=1}} = r_{L_{k=2}} = r_{L_{j=1}} = r_{L_{j=2}} = 1m\Omega$ $r_{in_{k=1}} = r_{in_{k=2}} = 1m\Omega$ $L_{k=1} = L_{k=2} = L_{j=1} = L_{j=2} = 1mH$ $D_{k=1} = D_{k=2} = (1 - \frac{E}{V_{bus}})$ and $D_{j=1} = D_{j=2} = \frac{V_o}{V_{bus}}$	Fig. 6.4 (a)	$2\omega-$ripple reduces in input current of first upstream converter, $k = 1$
Variation in output capacitance of each converter (C_{o_k} and C_{o_j})	Variable parameter: $C_{o_{k=1}} = C_{o_{k=2}} = C_{o_{j=1}} = C_{o_{j=2}} = 2\mu F,\ 22\mu F,\ 0.22mF,\ 2.2mF$ Fixed parameters: $C_{in_{k=1}} = C_{in_{k=2}} = C_{in_{j=1}} = C_{in_{j=2}} = 1mF$ $r_{L_{k=1}} = r_{L_{k=2}} = r_{L_{j=1}} = r_{L_{j=2}} = 1m\Omega$ $r_{in_{k=1}} = r_{in_{k=2}} = 1m\Omega$ $L_{k=1} = L_{k=2} = L_{j=1} = L_{j=2} = 1mH$ $D_{k=1} = D_{k=2} = (1 - \frac{E}{V_{bus}})$ and $D_{j=1} = D_{j=2} = \frac{V_o}{V_{bus}}$	Fig. 6.4 (b)	Negligible effect on $2\omega-$ripple
Variation in inductance of each converter (L_k and L_j)	Variable parameter: $L_{k=1} = L_{k=2} = L_{j=1} = L_{j=2} = 1mH,\ 3mH,\ 5mH,\ 7mH$ Fixed parameters: $C_{in_{k=1}} = C_{in_{k=2}} = C_{in_{j=1}} = C_{in_{j=2}} = 1mF$ $C_{o_{k=1}} = C_{o_{k=2}} = C_{o_{j=1}} = C_{o_{j=2}} = 1mF$ $r_{L_{k=1}} = r_{L_{k=2}} = r_{L_{j=1}} = r_{L_{j=2}} = 1m\Omega$ $r_{in_{k=1}} = r_{in_{k=2}} = 1m\Omega$ $D_{k=1} = D_{k=2} = (1 - \frac{E}{V_{bus}})$ and $D_{j=1} = D_{j=2} = \frac{V_o}{V_{bus}}$	Fig. 6.4 (c)	$2\omega-$ripple reduces in input current of first upstream converter, $k = 1$
Variation in parasitic resistance of inductor of each converter (r_{L_k} and r_{L_j})	Variable parameter: $r_{L_{k=1}} = r_{L_{k=2}} = r_{L_{j=1}} = r_{L_{j=2}} = 1m\Omega,\ 10m\Omega,\ 100m\Omega,\ 1000m\Omega$ Fixed parameters: $C_{in_{k=1}} = C_{in_{k=2}} = C_{in_{j=1}} = C_{in_{j=2}} = 1mF$ $C_{o_{k=1}} = C_{o_{k=2}} = C_{o_{j=1}} = C_{o_{j=2}} = 1mF$ $r_{in_{k=1}} = r_{in_{k=2}} = 1m\Omega$ $L_{k=1} = L_{k=2} = L_{j=1} = L_{j=2} = 1mH$ $D_{k=1} = D_{k=2} = (1 - \frac{E}{V_{bus}})$ and $D_{j=1} = D_{j=2} = \frac{V_o}{V_{bus}}$	Fig. 6.4 (d)	Negligible effect on $2\omega-$ripple

In the next Section, a phase-shift based ripple control technique is discussed.

6.5 PHASE-ADJUSTMENT BASED RIPPLE CONTROL

A typical DC microgrid has multiple sources, loads and storage interconnected through power converters. The single-phase inverters are generally used to converter the DC power into AC power in such systems. In such case, a large $2\omega-$ripple is reflected at the DC bus by the multiple inverter loads when supplied by DC bus. An additive effect of $2\omega-$ripple (when all ripples are in phase, see Fig. 6.5) further proliferates the $2\omega-$ripple problem. Therefore, a control technique is required to minimize $2\omega-$ripple at the DC bus. In this Section, a phase-adjustment based ripple control technique is presented for the off-grid DC microgrid having two inverter loads connected in parallel at the DC bus. To achieve the ripple reduction at the DC bus, a desired phase-shift (say ϕ) is created between the output AC voltages of inverters. In Fig. 6.5, the principle of ripple minimization at the DC bus is depicted for unity power factor inverter loads and different values of ϕ.

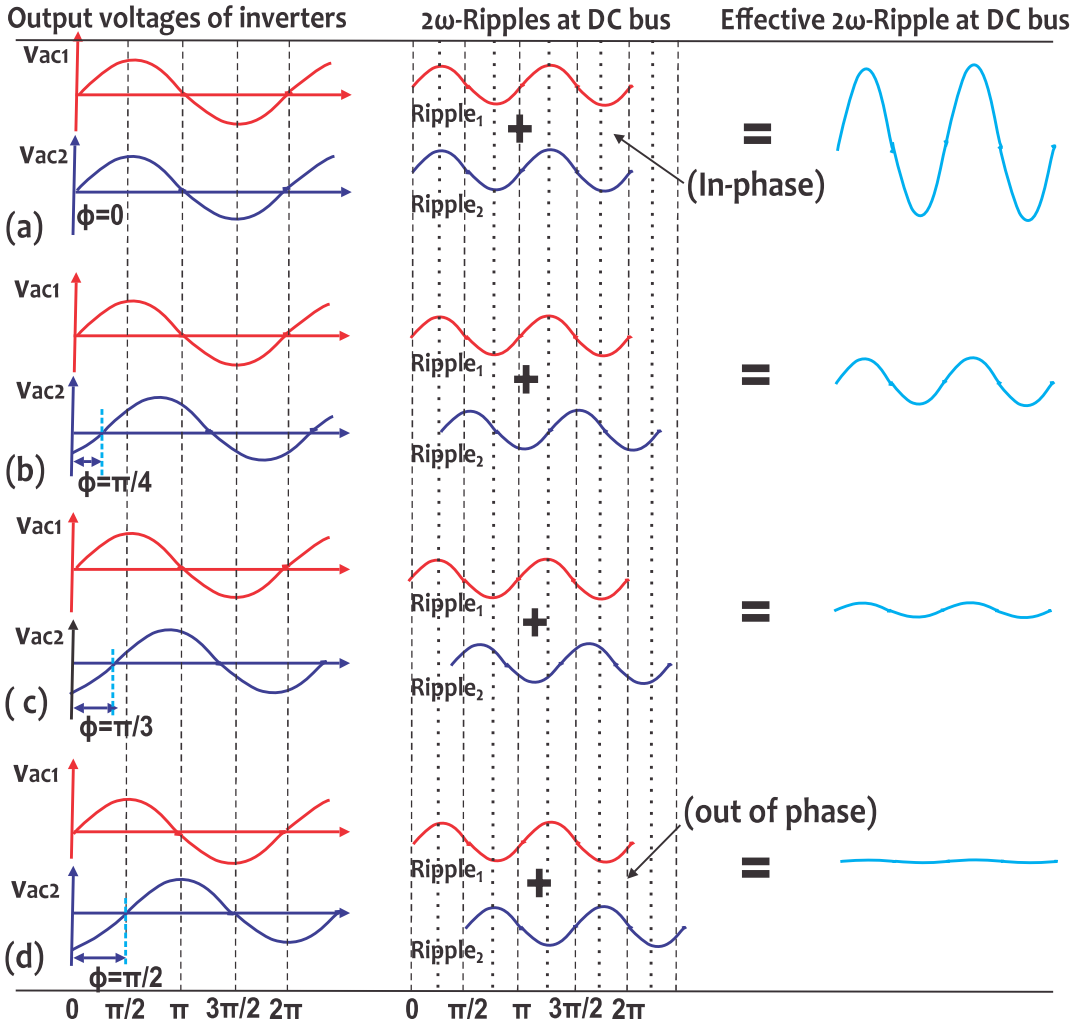

Figure 6.5 : Principle of phase-adjustment based ripple control: (a) for $\phi = 0$ ($2\omega-$ripples add to give large 2ω-ripple at the DC bus) (b) for $\phi = \pi/4$ (c) for $\phi = \pi/3$ (d) for $\phi = \pi/2$ (ripples cancel each other to minimum value)

Fig. 6.6 shows the circuit diagram of system having two inverter loads connected at the

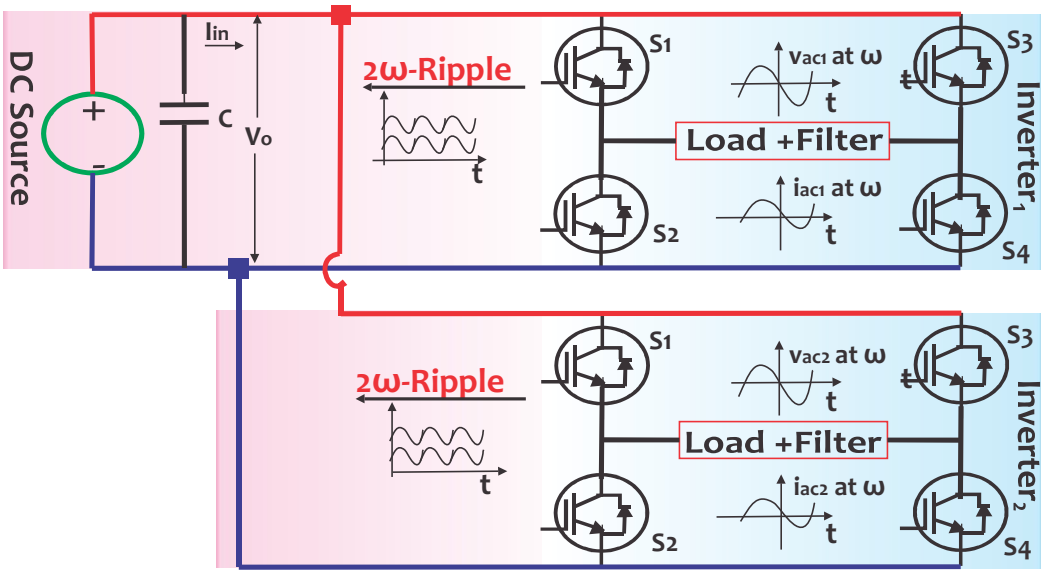

Figure 6.6 : Circuit Diagram

DC bus. To comprehend the concept of ripple minimization through the phase-adjustment based ripple control, suppose, in the Fig. 6.6, the output voltages and output currents of the two inverters are as follows,

$$v_{ac1} = V_{max1}cos(\omega t) \tag{6.27a}$$
$$i_{ac1} = I_{max1}cos(\omega t - \theta_1) \tag{6.27b}$$

and,

$$v_{ac2} = V_{max2}cos(\omega t) \tag{6.28a}$$
$$i_{ac2} = I_{max2}cos(\omega t - \theta_2) \tag{6.28b}$$

Here, v_{ac1} and v_{ac2} are the instantaneous output voltages of inverters. The angles θ_1 and θ_2 are the power factor angles. The subscript *max* stands for maximum value. Suppose M_1 and M_2 are modulation indices of inverters and V_o is the average value of the DC-link voltage. This implies $V_{max1} = M_1V_o$ and $V_{max2} = M_2V_o$. Further suppose the angle ϕ is the phase shift between instantaneous output voltages (v_{ac1}, v_{ac2}), and p_1 and p_2 are the instantaneous values of power of the inverters which are as follows,

$$p_1 = M_1V_ocos(\omega t + \phi)I_{max1}cos(\omega t + \phi - \theta_1) \tag{6.29a}$$
$$p_2 = M_2V_ocos(\omega t)I_{max2}cos(\omega t - \theta_2) \tag{6.29b}$$

Simplifying (6.29) gives,

$$p_1 = 0.5M_1V_oI_{max1}[cos\theta_1 + cos(2\omega t + 2\phi - \theta_1)] \tag{6.30a}$$
$$p_2 = 0.5M_2V_oI_{max2}[cos\theta_2 + cos(2\omega t - \theta_2)] \tag{6.30b}$$

For the ideal converters, the total power supplied to inverters at the DC bus is,

$$p_{Total} = p_1 + p_2 = 0.5V_o[M_1I_{max1}(cos\theta_1 + cos(2\omega t + 2\phi - \theta_1)) + M_2I_{max2}(cos\theta_2 + cos(2\omega t - \theta_2))]$$

(6.31)

The $2\omega-$ripple component in (6.31) is,

$$p_{ripple} = 0.5V_o[M_1 I_{max1} cos(2\omega t + 2\phi - \theta_1) + M_2 I_{max2} cos(2\omega t - \theta_2)] \tag{6.32}$$

The power ripple, p_{ripple} is the total $2\omega-$ripple reflected at the DC bus by the two inverters. The main objective is to minimize p_{ripple}, for this the control parameter i.e. phase-shift angle (ϕ) is adjusted accordingly. To find the angle ϕ for which the value of p_{ripple} is minimum, the first derivative of the (6.32) is,

$$\frac{dp_{ripple}}{d\phi} = -V_o M_1 I_{max1} sin(2\omega t + 2\phi - \theta_1) \tag{6.33}$$

For $\frac{dp_{ripple}}{d\phi} = 0$, the value of $2\omega t + 2\phi - \theta_1$ is $n\pi$, here n is an integer. Therefore, for $\omega t = 0$, the angle $\phi = \frac{n\pi+\theta_1}{2}$ rad/s. Now, to check the local maxima or minima at the angle $\phi = \frac{n\pi+\theta_1}{2}$ the second derivative is,

$$\frac{d^2 p_{ripple}}{d\phi^2} = -2V_o M_1 I_{max1} cos(2\omega t + 2\phi - \theta_1) \tag{6.34}$$

Substituting $\phi = \frac{n\pi+\theta_1}{2}$ in (6.34) gives,

$$\frac{d^2 p_{ripple}}{d\phi^2} = -2V_o M_1 I_{max1} cos(2\omega t + n\pi) \tag{6.35}$$

At $\omega t = 0$, the value of $\frac{d^2 p_{ripple}}{d\phi^2}$ is positive for $n = 2m \pm 1$, here $m = 0, 1, 2, 3...$ This implies that the value of p_{ripple} is minimum at $\phi = \frac{(2m\pm1)\pi+\theta_1}{2}$ rad/s. For $m = 0$ and $\theta_1 = 0$, the angle $\phi = \pm\frac{\pi}{2}$ rad/sec. Also, for $0 < \phi \leq \frac{\pi}{2}$, the value of effective ripple decreases with the increase in the value of ϕ and for $-\frac{\pi}{2} \leq \phi < 0$, the value of effective ripple decreases with the decrease in the value of ϕ. The effective value of the ripple is minimum at $-\frac{\pi}{2}$ or $\frac{\pi}{2}$ rad/sec.

It is to be noted that for $M_1 I_{max1} \neq M_2 I_2$, there will be always ripple irrespective of $\phi = \frac{n\pi+\theta_1}{2}$, however, the effective ripple will be minimum. The effective ripple can further be minimized up to some extent by adjusting modulation indice of the inverters for different values of I_{max} such that $M_1 I_{max1} \approx M_2 I_{max2}$. It is advised to keep modulation indices within the linear-range, generally preferred between 0.8 to 1 to keep desired level of THD. It is assumed here that the values of power factor angle are available to designer in order to implement this scheme of the phase-adjustment control.

6.5.1 Simulation Results

In this Section, the simulation results are presented for the system shown in Fig. 6.6. The simulation results are shown for two different cases: (a) $M_1 = M_2$ and $I_{max1} = I_{max2}$ (b) $M_1 \neq M_2$ and $I_{max1} \neq I_{max2}$ while $M_1 I_{max1} \approx M_2 I_{max2}$.

Case-I: $I_{max1} = I_{max2}$ **and** $M_1 = M_2$

(a) With unity power factor loads: The simulation results are shown in Fig. 6.7. The DC-link voltage, $V_o = 380\ V$, the modulation indice, $M_1 = M_2 = 0.8$ and $I_{max1} = I_{max2} = 5\ A$. In this case, the power factor angles are $\theta_1 = \theta_2 = 0$ and the phase shift angle ϕ is varied from 0^o to 90^o in the interval of 30^o. The $2\omega-$ripples in input current and DC-link voltage reduce to very low value at $\phi = 90^o$.

(b) With an inductive load at the first inverter and resistive load at the second inverter: The simulation results are shown in Fig. 6.8 for $\theta_1 = 48^o$ (lagging) and $\theta_2 = 0^o$. The DC-link voltage, $V_o = 380\ V$, the modulation indice, $M_1 = M_2 = 0.8$ and $I_{max1} = I_{max2} = 14\ A$. In this case, the angle

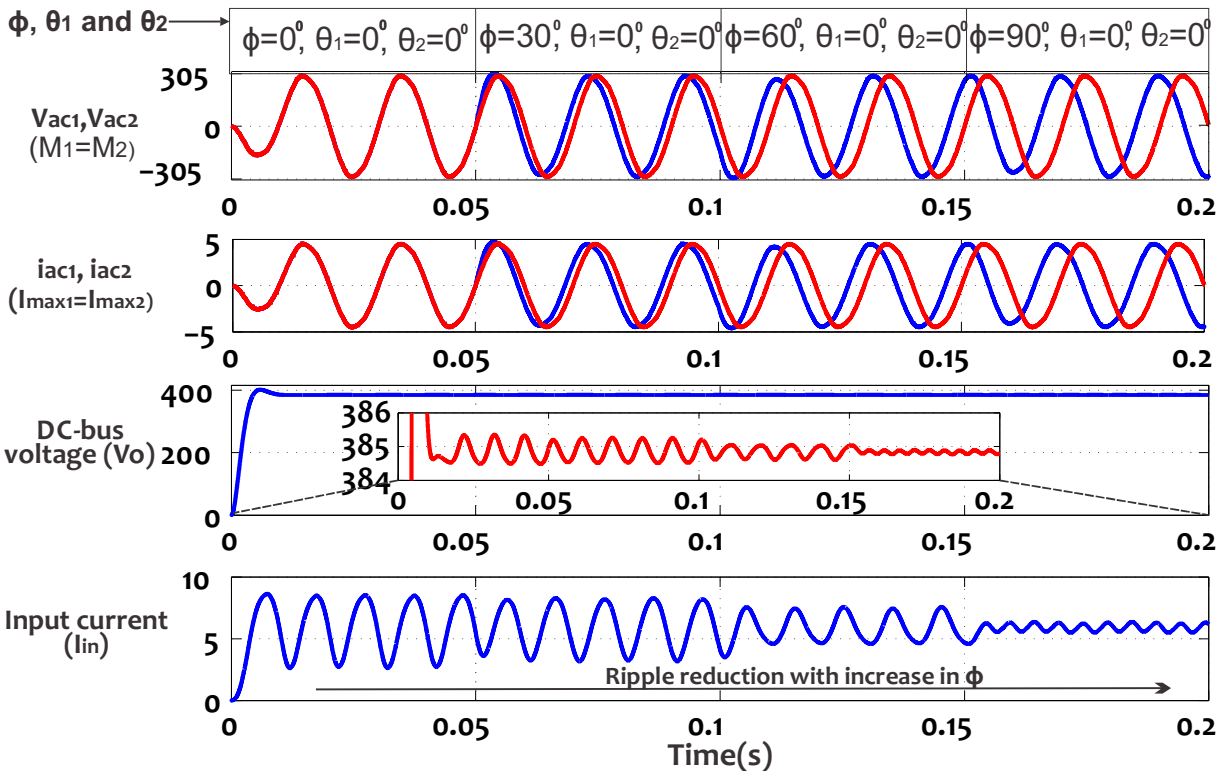

Figure 6.7 : Effect of phase-shift (ϕ) on $2\omega-$ripple for unity power factor inverter loads keeping $I_{max1} = I_{max2}$ and $M_1 = M_2$

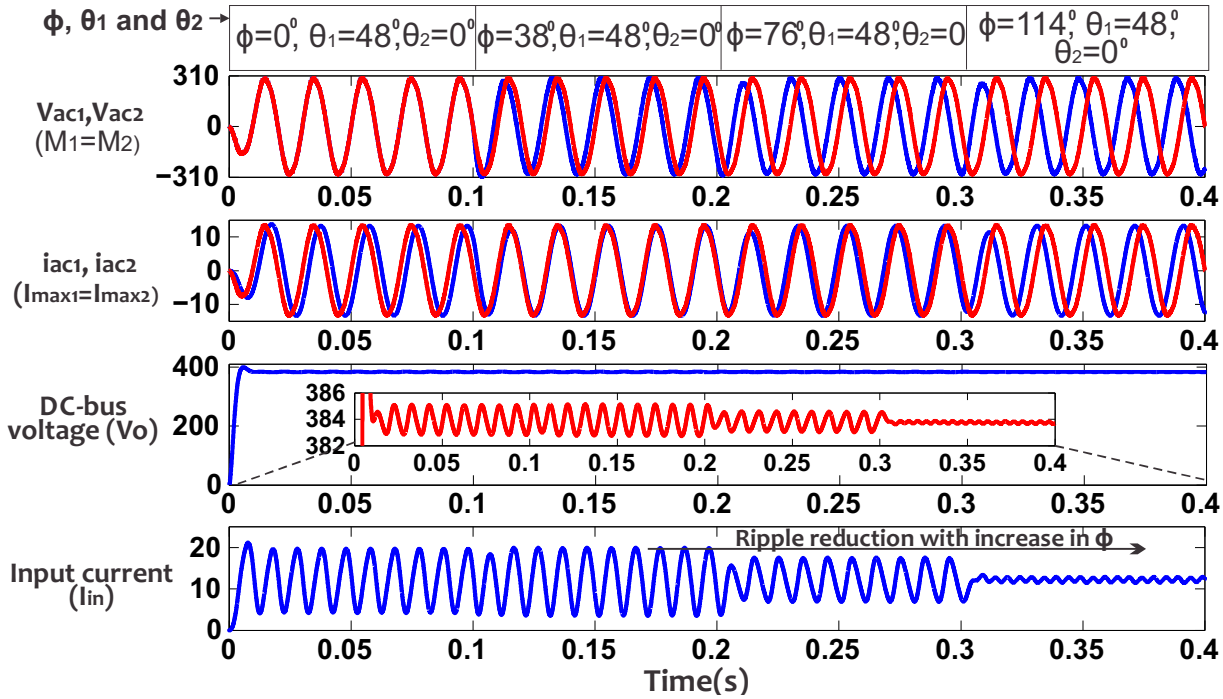

Figure 6.8 : Effect of phase-shift (ϕ) on $2\omega-$ripple for an inductive load at first inverter and resistive load at second inverter keeping $I_{max1} = I_{max2}$ and $M_1 = M_2$

ϕ is varied from 0^o to $90^o + (48^o/2) = 114^o$. The $2\omega-$ripples in input current and DC-link voltage reduce to very low value at $\phi = 114^o$.

Case-II: $I_{max1} \neq I_{max2}$ **and** $M_1 \neq M_2$

The simulation results are shown in Fig. 6.9 for $I_{max1} \neq I_{max2}$ and $M_1 \neq M_2$. In this case, the power factor angles are $\theta_1 = 58^o$ and $\theta_2 = 0$. In Fig. 6.9, the simulation results shown for the interval $0\ s$ to $0.2\ s$ are for $M_1 = M_2 = 0.8$ and $\phi = 90^o + (58^o/2) = 119^o$. In this interval, the value of $I_{max1} = 10\ A$ is less than $I_{max2} = 15\ A$. Therefore, the effective ripple is still large in the input current and DC-link voltage. To reduce the $2\omega-$ripple further, the modulation index M_1 is increased from $M_1 = 0.8$ to $M_1 = 0.95$ between the time interval $0.2\ s$ to $0.4\ s$ (see Fig. 6.9) such that the condition $M_1 I_{max1} \approx M_2 I_{max2}$ is followed that leads to maximum ripple-cancellation at DC-link. Hence, the value of the effective ripple is lesser for $M_1 = 0.95$ in comparison to $M_1 = 0.8$, however the magnitude of v_{ac1} increases due to increase in the modulation index.

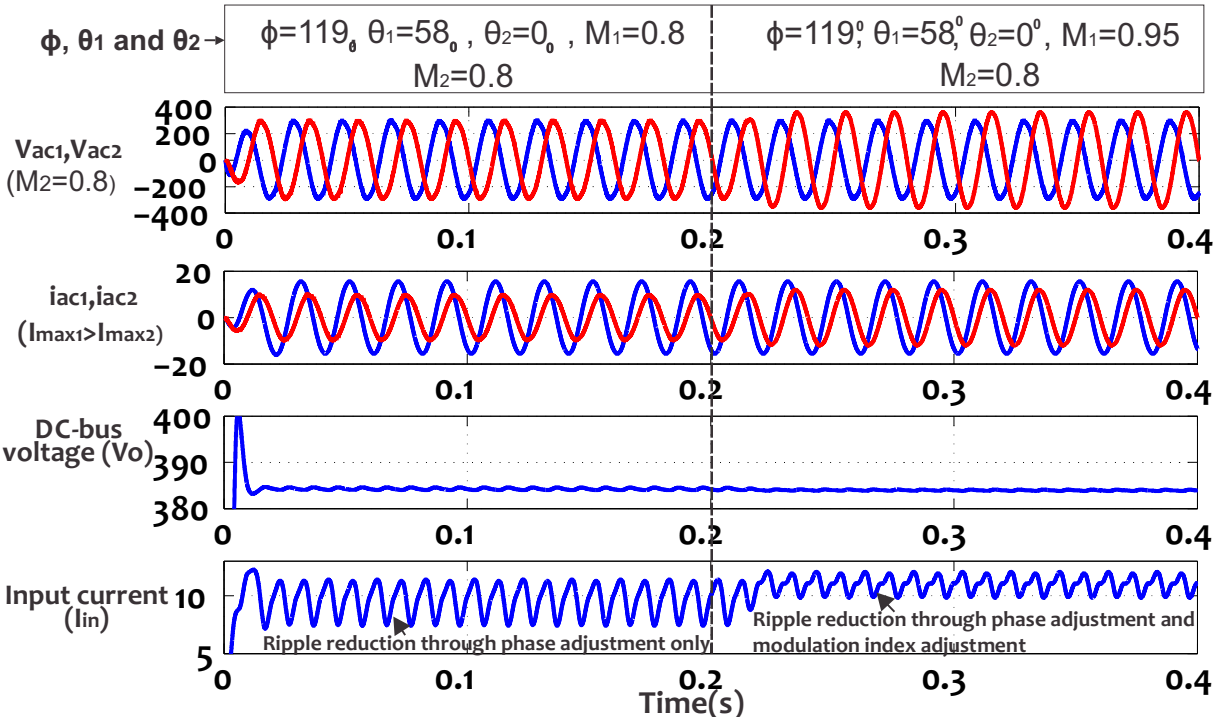

Figure 6.9 : Effect of phase-shift (ϕ) and change in modulation index on $2\omega-$ripple

6.6 SUMMARY

In this Chapter, a detailed analysis of the DC-microgrid have been presented in the context of $2\omega-$ripple. The effect of different system parameters on the $2\omega-$ripple is investigated using Bode plot technique. Furthermore, a phase-adjustment based ripple control technique has been presented using two inverert loads with different loading conditions. A desired phase-shift angle between the output voltages of the inverters minimizes the ripple at DC link. In the next Chapter, the conclusion of this Thesis work and future challenges and scopes will be discussed.